Magnetization reversal in (Ga,Mn)As/MnO exchange-biased structures: Investigation by planar Hall effect

Z. Ge, W. L. Lim, S. Shen, Y. Y. Zhou, X. Liu, J. K. Furdyna, and M. Dobrowolska*
Department of Physics, University of Notre Dame, Notre Dame, Indiana 46556, USA
(Received 6 September 2006; revised manuscript received 10 November 2006; published 8 January 2007)

The asymmetric planar Hall effect (PHE) has been investigated in a series of (Ga,Mn)As/MnO ferromagnetic-antiferromagnetic bilayer structures, all of which exhibit exchange bias (EB) up to 140 Oe as determined by direct magnetization measurements. The reversal of in-plane magnetization in these structures was systematically studied by the angular dependence of PHE with respect to the direction of the applied magnetic field. The behavior of PHE in structures with EB is very different from the PHE results observed on typical (Ga,Mn)As layers with no antiferromagnetic capping. In particular, in field-cooled experiments on (Ga,Mn)As/MnO we observe asymmetry in the PHE resistance upon reversal of the applied magnetic field when the field is swept along the direction of the cooling field. Analysis of the experimental results based on the Stoner-Wohlfarth model (including domain nucleation and expansion in the ferromagnetic layer) reveals that in EB systems magnetization reversal can occur via two paths: the magnetization undergoes either a full circle rotation or a half circle rotation as the field is reversed, depending on the direction of the applied field relative to the cooling field. Our model is confirmed by the close agreement of its theoretical prediction with the experimental data.

DOI: 10.1103/PhysRevB.75.014407 PACS number(s): 75.70.−i, 75.50.Pp, 75.60.Jk, 75.70.Cn

I. INTRODUCTION AND BACKGROUND

Exchange coupling between adjacent ferromagnetic (FM) and antiferromagnetic (AF) layers was discovered approximately four decades ago in Co-CoO bilayers.[1] The effect manifests itself by several characteristic features, among which the most well known is the shift of the center of magnetization hysteresis loop away from zero field [referred to as exchange bias (EB)], and an accompanying enhancement of magnetic coercivity. Since such exchange bias can be applied in giant magnetoresistance spin-valve heads for high-density recording systems,[2] the interest in this effect is intense. A comprehensive review of the subject, which emphasizes experimental results and provides a list of relevant publications, was published by Nogués and Schuller.[3] Furthermore, the article by Kiwi[4] is recommended for investigators interested in theoretical models describing the exchange bias phenomenon. These models are briefly summarized below.

Basically, when we are dealing with the exchange biased systems, we assume an uncompensated interface, which means that there exist uncompensated spins at the interface due to field cooling. This has been discussed in detail by Stiles and McMichael,[5] and has successfully explained experimental data in many structures.[6] By assuming an uncompensated interface, the picture of exchange bias can be further simplified by treating the AF layer as a single-domain system having an anisotropy that is established along the cooling field direction during field cooling.[1] This approach, however, is not regarded as sufficient, since it relies on an unrealistically perfect interface, and it predicts the magnitude of exchange bias to be several orders of magnitude larger than what is observed experimentally.

Mauri *et al.* developed a more realistic model,[7] which predicts a smaller value of exchange bias by introducing domain walls in the AF layer parallel to the layer plane. In this model the interfacial coupling energy can spread into the entire AF layer via domain wall formation. Unfortunately, this model fails to explain the persistence of exchange bias down to very small thicknesses of the AF layer (e.g., 25 Å); and it also assumes a perfect interface. Xi and White[8] analyzed Mauri *et al.*'s model as a function of AF layer thickness t_{AF}, and showed that this model can also explain coercivity enhancement (at least partially) by possible transitions of AF spins between their two degenerate states. In another approach, Malozemoff introduced a model that additionally includes domain walls perpendicular to the plane of the AF layer, which can arise, e.g., from the inevitable roughness of the interface.[9] In this model (called the random field model) the exchange coupling energy is averaged in each AF domain, which results in a smaller exchange bias as compared to that calculated by assuming a single domain in the AF layer. The domain structure in the AF layer was experimentally proved to be important in exchange biased systems by Miltényi *et al.*,[10] who found that one can control the properties of the exchange bias field by intentionally diluting the AF layer. Moreover, such a random field situation can locally pin FM moments, impeding their freedom to rotate as the magnetic field is swept, thus leading to an increase in the coercivity.[11–13] Compared to other models, the random field theory is more realistic, since a perfectly uncompensated interface can seldom be found in real systems.

We finally mention the model proposed by Stiles and McMichael[14] who, by combining the planar domain wall model and the random field model, showed that the enhancement of the coercivity can originate both from irreversible transitions of AF spins (which prevail at elevated temperatures) and from inhomogeneous reversal of FM moments (which exists at all temperatures). The increasingly sophisticated models listed above have been the primary theoretical tools invoked in dealing with the two signatures of exchange biased systems: the conspicuous shift of the hysteresis loop, and the enhancement of the coercivity.

Experimentally, various systems comprised of different AF and FM materials have been studied, and much detailed information can be found in Ref. 3, along with examples of many structures in which exchange bias was investigated. One should note, however, that most of the systems employed to date involved metallic FM materials. On the other hand, since ferromagnetic semiconductors such as (Ga,Mn)As have been the subject of extensive experimental and theoretical research for nearly a decade,[15–17] and the magnetic anisotropy associated with this material is rather complicated,[18,19] it appears important to look into the behavior of EB in systems where (Ga,Mn)As is the FM layer. Early attempts to look for EB in (Ga,Mn)As layers were made by Liu and Furdyna *et al.*,[20,21] using either ZnMnSe or MnTe as AF capping layers. In these studies only one of the signatures characteristic of exchange biased systems—the enhancement of the coercivity—has been observed. The failure to detect an EB field (i.e., the shift of the hysteresis loop from zero field) was ascribed in those studies to the large thickness of the FM layer (~300 nm) and to the small magnetic anisotropy of the AF layer. More recently, bilayer structures composed of relatively thin layers (~10 nm) of (Ga,Mn)As and of antiferromagnetic MnO have been studied by Eid *et al.*,[22] who observed a substantial EB field (up to 200 Oe) in this system. Their work demonstrated that, to observe the EB field, systematic post-growth treatment of the FM-AF bilayers is essential.

The EB field can be determined either by direct measurement of magnetization, or indirectly from magnetotransport measurements, e.g., from the anisotropic magnetoresistance,[23–25] anomalous Hall effect,[25] or the planar Hall effect (PHE).[26] Due to its relationship to the direction of magnetization, PHE measurements offer a particularly powerful tool for probing the process of magnetization reversal. In the *standard* Hall-bar configuration the electric field ϵ_y perpendicular to the current, which determines PHE, is given by[27]

$$\epsilon_y = \tfrac{1}{2} j(\rho_{\parallel} - \rho_{\perp})\sin(2\varphi_F), \tag{1}$$

where j is the current density, $\rho_{\parallel}$ and $\rho_{\perp}$ are resistivities parallel and perpendicular to the current, respectively, and φ_F indicates the direction of magnetization **M** in the FM layer relative to the current. In our system the measured signal, i.e., the PHE resistance, can be written as

$$R_{\mathrm{PHE}} = \frac{l\epsilon_y}{Sj} \equiv -R_{\mathrm{Amp}}\sin(2\varphi_F), \tag{2}$$

where l and S are the length and the cross-sectional area of the Hall bar, respectively, and $R_{\mathrm{Amp}} = -l(\rho_{\parallel} - \rho_{\perp})/2S$ is the amplitude of the PHE resistance. The giant PHE in (Ga,Mn)As epilayers was first observed by Tang *et al.*,[28] and subsequently Lim *et al.*[29] studied PHE in samples grown on tilted substrates in which it was shown that the magnetization reversal occurs in a preferred crystalline plane rather than in the sample plane.

Generally the process of magnetization reversal in (Ga,Mn)As involves an intermediate step in which the FM domain switches its orientation by 90°, causing ϵ_y to flip its sign when such a switching occurs [see Eq. (1)]. This provides the ability to monitor the magnetization reversal process in a more detailed way than is possible in conventional magnetization measurements, since direct measurements of magnetization are only sensitive to the projection of **M** on **H** (i.e., they are insensitive to such intermediate steps as just described).

II. SAMPLE FABRICATION AND EXPERIMENTAL PROCEDURE

A series of (Ga,Mn)As/MnO bilayer structures was grown by molecular beam epitaxy (MBE) on (001) semi-insulating GaAs substrates in a Riber 32 R&D MBE system. The MBE growth was monitored by reflection high energy electron diffraction (RHEED), and was carried out as follows. A GaAs buffer layer of 160 nm was first deposited on the substrate at a high temperature ($T_S \sim 600$ °C). The substrate was then cooled to 275 °C for low temperature (LT) growth, and a 2-nm-thick buffer layer of LT-GaAs was grown while keeping the As_2:Ga beam equivalent pressure ratio at 20:1. This was followed by the growth of (Ga,Mn)As layers with different thicknesses. The Mn concentration of the (Ga,Mn)As layers was estimated to be 4% for all samples by comparing the growth rates of LT-GaAs and (Ga,Mn)As, as measured by RHEED oscillations.[30] After (Ga,Mn)As deposition each sample was cooled to a low substrate temperature ($T_S \sim 19$ °C), and a Mn layer was deposited on the surface to a thickness of several nm.

After removal from the ultrahigh vacuum MBE chamber, the Mn capping layer was oxidized by heating each sample in air for several minutes in order to form MnO. The reason for doing this is that, although metallic Mn is an antiferromagnet, the presence of the Mn layer itself does not produce EB, as was shown by Eid *et al.*[22] It has therefore been concluded that oxidation of the Mn layer is critical for the observation of EB. Each sample in the series was oxidized in the same way. After oxidation x-ray reflectivity measurements are carried out on all samples to determine the thickness of the MnO layer t_{AF}. The results show that a ~15 nm MnO layer was achieved in each case, although its thickness is not perfectly uniform across the sample plane.[31]

Magnetization measurements were carried out on the samples described above using a commercial superconducting quantum interference device (SQUID) magnetometer, including measurements of both temperature and field dependence of magnetization for different directions of the cooling field. We compared the results for samples with different FM layer thicknesses, from which we selected the sample showing the largest EB, on which we performed PHE measurements at 4.2 K. For those studies the layer was cleaved into standard Hall bars with dimensions of 0.6 mm × 2 mm, the long side (which is also the direction of current flow) corresponding to the [110] direction. The directions of the cooling field and of the applied field were always in the plane of the film. The value of the cooling field applied as the sample was cooled from room temperature to 4.2 K was 0.10 T. After cooling, the PHE measurements were carried out with magnetic field applied along different directions and swept over a

field loop ranging between −0.20 T and +0.20 T. A program-controlled Keithley 220 current source was used to supply the current. As the field was swept out, transverse (Hall) and longitudinal voltages were measured simultaneously on the Hall bar by two Keithley digital multimeters. A program-controlled Lakeshore power supply provided a preset current sequence to the superconducting magnet for sweeping the field in the above measurements.

III. MODELING AND CALCULATIONS

A. Free energy of a (Ga,Mn)As/MnO bilayer

The simplest picture of an exchange-biased system is to assume a single domain FM layer, with frozen spins aligned along the cooling field direction in the AF layer. We will discuss the suitability of these assumptions for our structures. In the FM (Ga,Mn)As layer planar domain walls can be ignored, since the thickness of the FM layer is small ($t_F \sim 15$ nm) and the effect of interfacial coupling between the FM and AF layers is weak (i.e., it is only a perturbation to the reversal process of FM magnetization). Indeed, Refs. 32 and 33 predict that perpendicular domain wall thicknesses in thin (Ga,Mn)As are in the neighborhood of 15–30 nm. On the other hand, the effects of the possible perpendicular domain walls formed in the (Ga,Mn)As layer will be discussed later. In the AF layer, we must be cautious since planar domain walls,[7] perpendicular domain walls,[9] or both[14] may exist in this layer. To study the behavior of the EB field itself, it is sufficient to just consider the planar domain walls. The domains with domain walls perpendicular to the sample plane are mainly responsible for the coercivity enhancement, as suggested by Zhang *et al.* and Li and Zhang.[11–13] Such pinning effects on the FM layer arising from the AF layer have in fact already been observed experimentally by Leighton *et al.*[34]

The above simplifications allow us to treat the properties of the EB system in terms of an effective average interfacial coupling. The magnitude of this effective coupling is given by $J_E = -H_{\mathrm{EB}} M_S t_F$, where H_{EB}, M_S, and t_F are the EB field, the saturated magnetization, and the thickness of the (Ga,Mn)As layer, respectively. The validity of these approximations will be discussed *a posteriori* by the quality of the agreement between experimental data and the computed results.

In this spirit, the energy per unit area of the system should consist of three parts: the energy of the FM layer E_F; the energy of the AF layer E_{AF}; and the exchange coupling energy between the two layers, E_{int}:

$$E = E_F + E_{\mathrm{AF}} + E_{\mathrm{int}}. \tag{3}$$

We will discuss each of these energy terms in the subsections that follow.

1. Free energy of the FM layer (E_F)

The full expression for E_F in a zinc-blende crystal film such as (Ga,Mn)As in an applied dc magnetic field **H** is[18,35]

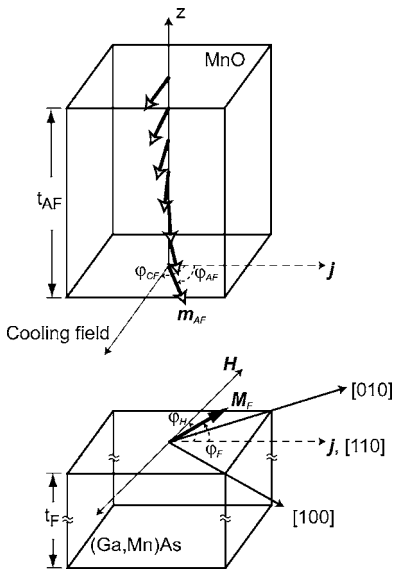

FIG. 1. Schematic of the (Ga,Mn)As/MnO exchange-biased bilayer and the coordinate system used in this article. Both the magnetic field applied during the measurements and the cooling field are in the sample plane. The current is along the [110] crystalline direction of the (Ga,Mn)As layer. The magnetic field used in the measurements is applied along different azimuthal angles φ_H relative to the current, while cooling field is fixed in the $[1\bar{1}0]$ crystalline direction of the (Ga,Mn)As layer. The possible winding of the spins in the AF layer along the normal to the sample plane (the z axis) direction is also shown.

$$\begin{aligned} E_F/t_F = &- MH[\cos\theta_F \cos\theta_H + \sin\theta_F \sin\theta_H \cos(\varphi_F - \varphi_H)] \\ &+ \left[2\pi M^2 - K_{2\perp} - \frac{1}{2}K_{4\perp}\cos^2\theta_F\right]\cos^2\theta_F \\ &- \frac{1}{2}K_{4\parallel}\frac{1}{4}\left\{3 + \cos\left[4\left(\varphi_F + \frac{\pi}{4}\right)\right]\right\}\sin^4\theta_F \\ &- K_{2\parallel}\sin^2\theta_F \sin^2\varphi_F. \end{aligned} \tag{4}$$

The meaning of each parameter in this equation is exactly the same as that in Ref. 18, and the azimuthal angles φ_F and φ_H are defined in Fig. 1. It can be readily shown that in the case of an in-plane magnetic field ($\theta_H = \pi/2$), for a sufficiently large value of $2\pi M - K_{2\perp}/M$ (as is the case in our system) $\theta_F = \pi/2$ corresponds to the stable angle of magnetization (i.e., the angle for which E_F is minimized), as can be verified by taking the first and second derivatives of E_F with respect to θ_F. The expression for E_F can then be simplified to a more compact form,

$$\frac{E_F}{t_F} = -MH\cos(\varphi_F - \varphi_H) + \frac{K_{4\parallel}}{8}\cos 4\varphi_F - K_{2\parallel}\sin^2\varphi_F, \tag{5}$$

where $K_{2\parallel}$ and $K_{4\parallel}$ are the in-plane uniaxial and cubic anisotropy energies, respectively.

2. Free energy of the AF layer (E_{AF})

We now consider the AF MnO capping layer. We have neglected perpendicular domain walls in the MnO film by assuming a uniform effective interfacial coupling. In this situation, it is best to further simplify the model by neglecting the movement of AF spins during the reversal of FM magnetization, thus allowing us to ignore the contribution to the free energy from the AF layer. To check this, we will estimate the deviation of AF spins from the cooling field direction by two approaches: first, by assuming a single domain structure in the AF layer; and second, by assuming a planar domain structure in that layer. This requires us to know the values of the anisotropy constant K_{AF} and the exchange stiffness A_{AF} of the AF layer, which will be given in Sec. IV B. Since the planar domain wall approach is an approximation compatible with very large t_{AF}, while the single-domain assumption is suitable for small t_{AF}, the actual deviation for realistic values of t_{AF} should lie between the values obtained by these two approaches.

Using the single domain approximation for the AF layer, it can be readily shown that the magnetic anisotropy energy in the AF layer is given by[1]

$$E_{\mathrm{AF}} = K_{\mathrm{AF}} t_{\mathrm{AF}} \sin^2(\varphi_{\mathrm{AF}} - \varphi_{\mathrm{CF}}). \tag{6}$$

By combining this with the total free energy equation for the whole system, we can then estimate the maximum deviation $|\varphi_{\mathrm{AF}} - \varphi_{\mathrm{CF}}|$ of the AF spins from the cooling field direction in the single AF domain limit.

On the other hand, in the approach which we refer to as the planar domain wall model, the total energy in the AF layer can be written as[36,37]

$$E_{\mathrm{AF}} = \int_0^{t_{\mathrm{AF}}} \left[A_{\mathrm{AF}} \left(\frac{d\Phi_{\mathrm{AF}}(z)}{dz} \right)^2 + K_{\mathrm{AF}} \sin^2(\Phi_{\mathrm{AF}}(z) - \varphi_{\mathrm{CF}}) \right] dz, \tag{7}$$

which for large t_{AF} becomes

$$E_{\mathrm{AF}} = \sigma_w [1 - \cos(\varphi_{\mathrm{AF}} - \varphi_{\mathrm{CF}})], \tag{8}$$

where $\sigma_w = 2\sqrt{A_{\mathrm{AF}} K_{\mathrm{AF}}}$ is the domain wall energy characteristic of the AF layer. This planar domain wall approach can then be used to obtain a corresponding maximum deviation from the cooling field direction of the AF moments at the interface.

The actual maximum deviation of the AF moments at the interface will be estimated in Sec. IV B, after the values of the relevant parameters are established. The magnitude of this deviation will then indicate whether or not we can simplify the problem by neglecting the movement of AF spins.

3. Interfacial coupling energy between FM and AF layers (E_{int})

The third term in Eq. (2), i.e., the exchange coupling energy between FM and AF layers, can be readily shown to be

$$E_{\mathrm{int}} = -J_E \cos(\varphi_F - \varphi_{\mathrm{AF}}), \tag{9}$$

where J_E is the effective exchange coupling constant between adjacent FM and AF grains, experimentally given by $J_E = -H_{\mathrm{EB}} M_S t_F$. One must note that the value of J_E so obtained might not be the actual value of the local exchange coupling between FM and AF spins.

With this, we can finally write expressions for the total energy per unit area of the system for the two limiting cases, i.e., for the case of a single-domain AF layer, and for the planar domain wall approach. The single-domain model gives

$$E = t_F \left[-MH \cos(\varphi_F - \varphi_H) + \tfrac{1}{8} K_{4\parallel} \cos 4\varphi_F - K_{2\parallel} \sin^2 \varphi_F \right] - J_E \cos(\varphi_F - \varphi_{\mathrm{CF}}) + K_{\mathrm{AF}} t_{\mathrm{AF}} \sin^2(\varphi_{\mathrm{AF}} - \varphi_{\mathrm{CF}}); \tag{10a}$$

and when planar domain walls are assumed, we have

$$E = t_F \left[-MH \cos(\varphi_F - \varphi_H) + \tfrac{1}{8} K_{4\parallel} \cos 4\varphi_F - K_{2\parallel} \sin^2 \varphi_F \right] - J_E \cos(\varphi_F - \varphi_{\mathrm{CF}}) + \sigma_w [1 - \cos(\varphi_{\mathrm{AF}} - \varphi_{\mathrm{CF}})]. \tag{10b}$$

We will use these two equations in Sec. IV B to estimate the upper and lower limits for the maximum deviation of the interfacial AF moments relative to the cooling field direction. As will be seen, this will provide justification for neglecting the movement of AF spins during magnetization reversal in the (Ga,Mn)As/MnO bilayers of interest in this paper.

B. Algorithm for simulating magnetization reversal

Generally a configuration of the FM-AF system given by a pair of angles $(\varphi_F, \varphi_{\mathrm{AF}})$ will be stable when it corresponds to a minimum of the total free energy, i.e., when the following conditions are satisfied:

$$\frac{\partial E}{\partial \varphi_F} = 0, \quad \frac{\partial E}{\partial \varphi_{\mathrm{AF}}} = 0,$$

$$\frac{\partial^2 E}{\partial^2 \varphi_F} > 0, \quad \frac{\partial^2 E}{\partial^2 \varphi_{\mathrm{AF}}} > 0,$$

$$\frac{\partial E}{\partial \varphi_F} \frac{\partial E}{\partial \varphi_{\mathrm{AF}}} - \frac{\partial^2 E}{\partial \varphi_F \partial \varphi_{\mathrm{AF}}} > 0.$$

In later discussion we will show that for our system comprised of MnO and (Ga,Mn)As layers we are safe to disregard the changes in φ_{AF}.

In particular, in the (Ga,Mn)As layer we also take into account the fact that the process of magnetization reversal is assisted by domain nucleation and domain wall movement.[28,38] When the difference between the free energies of two neighboring local minima is sufficiently large ($\geqslant E_{\mathrm{DW}}$, the energy for the formation of domain walls), domains with magnetization along the easier direction will nucleate and rapidly expand. In the simulation, we treat this situation as if the magnetization undergoes an abrupt jump between the "less easy" and the "more easy" direction. Note, however, that this single domain model in (Ga,Mn)As has more recently been questioned under certain conditions by another group of authors,[39] and we will discuss this issue later in this paper.

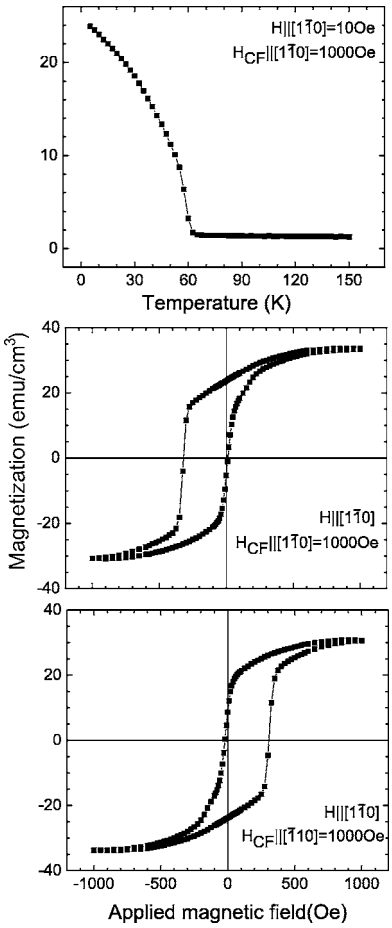

FIG. 2. Magnetization results obtained on the (Ga,Mn)As/MnO bilayer using SQUID measurements with directions of the cooling field H_{CF} and the applied field H indicated in each panel. (a) Temperature dependence of the magnetization measured in a small applied magnetic field (10 Oe). (b) Low temperature (T=5 K) magnetization as a function of the applied magnetic field, observed after a cooling field of 1000 Oe was applied along the [1$\bar{1}$0] direction of the (Ga,Mn)As. (c) Low temperature (T=5 K) magnetization as a function of the applied magnetic field, observed after a cooling field of −1000 Oe along the [$\bar{1}$10] direction. Positive values of H correspond to the [1$\bar{1}$0] direction.

IV. RESULTS AND DISCUSSION

A. Magnetization results

SQUID magnetization data obtained on the sample with t_F=15 nm (the specimen showing the largest exchange bias field H_{EB}) are shown in Fig. 2. The saturation magnetization M_S determined from the field dependence of these data is 32 emu/cm^3. The temperature dependence shown in Fig. 2(a) gives a Curie temperature $T_C \sim 60$ K for this sample. Thus T_C is in this case lower than the Néel temperature of MnO ($T_N \sim 110$ K), corresponding to the condition discussed in Ref. 40, which is an unconventional situation in typical exchange-biased systems. Systems with $T_N > T_C$ have, however, been studied experimentally by Wu and Chien,[41] who argued convincingly that the magnetization above T_C of the FM layer induced by the cooling field is already sufficient to establish exchange coupling. On the other hand, the temperature dependence data of the EB field[42] show that, although the blocking temperature T_B (above which the EB field vanishes) of our structure may vary with the grain size in the MnO layer, it is always lower than T_C. If we reverse the sign of the cooling field, as shown in Figs. 2(b) and 2(c), the sign of the exchange bias also changes, always remaining opposite to that of the cooling field. The exchange bias for this sample is determined to be approximately 140 Oe.

In addition, a clear asymmetry is observed for the decreasing and increasing sides of both hysteresis loops in Figs. 2(b) and 2(c). To facilitate discussion of the loops, we will designate the magnetic field sweep from negative maximum field to positive maximum field as the "increasing field branch;" and the sweep from positive maximum to negative maximum field will be referred to as the "decreasing field branch." It is seen that, for both directions of the cooling field, the branch whose field sweep direction is opposite to that of the cooling field has a sharp corner, while the other branch is rounded. A similar behavior has been reported by Fitzsimmons *et al.*,[43] and has subsequently been studied extensively by numerous authors (see, e.g., Refs. [44–49]). Different interpretations of the origin of this asymmetry were given, and it is commonly suggested that this asymmetry may be closely related to training effects of the EB field. Generally speaking, as the magnetic field is swept in the direction opposite to that of the cooling field, competition between inhomogeneous interfacial coupling and other fields (the applied magnetic field and the anisotropy fields) will lead to a multidomain state in the FM layer. However, when sweeping the field in the other direction, the interfacial coupling does not compete with the applied field due to the fact that the coupling is unidirectional. This asymmetry in the process of magnetization reversal manifests itself in the SQUID data as an asymmetry in the hysteresis loop.

B. Simulation parameters

In this section we collect the parameters appearing in Eqs. (10a) and (10b), to be used in simulations of the results obtained in this study. At low temperatures (to which we restrict ourselves in this paper) the effective interfacial coupling constant is given by $J_E = -H_{EB} M_S t_F$, where H_{EB}=140 Oe and M_S=30 emu/cm^3 are both obtained from the SQUID data, and t_F=15 nm is estimated from the growth rate and the growth time. In our simulation, the following material parameters were used for MnO: exchange coupling constant $J_{AF}/k_B \sim 11.3$ K,[50] where k_B is the Boltzmann constant; exchange stiffness $A_{AF} \sim 2J_{AF}S^2/a = 4.37 \times 10^{-7}$ erg/cm, where S=5/2 is the spin of the Mn^{++} ions, and a=4.43 Å is the lattice parameter of MnO; anisotropy constant[51,52] $K_{AF} \sim 3.2 \times 10^4$ erg/cm^3; and domain wall energy $\sigma_w = 2\sqrt{A_{AF}K_{AF}} = 0.236$ erg/cm^2. The magnetic anisotropy constants used in the calculation for the (Ga,Mn)As layer were determined by ferromagnetic resonance measured on the same sample: $4\pi M_S - 2K_{2\perp}/M_S \approx 3396$ Oe, $2K_{4\perp}/M_S \approx 104$ Oe, $2K_{2\parallel}/M_S \approx 34$ Oe, and $2K_{4\perp}/M_S \approx 1268$ Oe. The value of the domain wall energy in the FM layer, E_{DW}, will be discussed separately in Sec. IV B 2.

Except for this last item, we thus have the values of all the parameters required for carrying out the simulation using Eqs. (10a) and (10b). The last question to verify is whether we can treat AF spins as frozen as noted at the end of Sec. III, where we anticipated that in our system it is justified to consider only the movement of magnetic moments in the FM layer. We will discuss this issue in the next subsection in the context of the parameters given above.

1. Can AF spins be treated as frozen spins?

Combining the values of J_E, σ_W, and K_{AF} given above, we are now able to assess the validity of the assumption of frozen AF spins mentioned in Sec. III A 2. By choosing appropriate reduced units, we can write the parameters as $\sigma_W/M_S t_F = 4920$ Oe and $K_{\mathrm{AF}}/M_S \sim 1000$ Oe, which lead to a physically clearer picture. In the single-domain approach [for which the total energy is given by Eq. (10a)], the condition $\partial E/\partial\varphi_{\mathrm{AF}}=0$ required by the minimization of energy yields the relation: $\sin[2(\varphi_{\mathrm{AF}}-\varphi_{\mathrm{CF}})]=-(J_E/K_{\mathrm{AF}}t_{\mathrm{AF}})\sin(\varphi_F-\varphi_{\mathrm{AF}})$. By recalling that in our system $t_F \approx t_{AF}$, the condition $|\sin[2(\varphi_{\mathrm{AF}}-\varphi_{\mathrm{CF}})]| \leqslant J_E/K_{\mathrm{AF}}t_{\mathrm{AF}}$ defines the maximum deviation of the AF spin orientation from the cooling field direction $|\varphi_{\mathrm{AF}}-\varphi_{\mathrm{CF}}|$ to be $\sim 4.6°$. Similarly, the maximum deviation obtained when one uses the planar domain wall approach [i.e., using the total energy given by Eq. (10b)] is found to be $\sim 1.9°$. The actual maximum deviation should then be between these two values, as discussed earlier. At this point we can therefore safely say that the simplification of the model by disregarding the movement of AF moments in the numerical simulation is indeed justified. Making this assumption, we can now write the equation for the energy of the system as

$$E = t_F\left[-MH\cos(\varphi_F-\varphi_H)+\tfrac{1}{8}K_{4\|}\cos 4\varphi_F - K_{2\|}\sin^2\varphi_F\right] - J_E\cos(\varphi_F-\varphi_{\mathrm{CF}}), \tag{10c}$$

which will be the expression for the total energy used later in this article for simulating the process of magnetization reversal.

We should note that no training effects were observed in our measurements of the hysteresis loop over the ±0.2 T cycle, which is consistent with the fact that the calculated value of the energy of AF domain wall $\sigma_W/M_S t_F = 4920$ Oe is larger than the maximum magnetic field. Nevertheless, when the range of the loop swept out by the field is increased to fields higher than ±0.6 T, a gradual decay in H_{EB} is observed in consecutive runs, showing that the training effect in our system is more likely caused by reorientation of AF spins by the applied magnetic field than by the interfacial coupling.[3]

2. Energy of domain wall formation E_{DW} in the FM layer

To determine the value of E_{DW}, we look at the experimental PHE data at $\varphi_H = 87.7°$ in Fig. 3(a), which illustrates the variation of experimental PHE curves with respect to the angle of applied magnetic field. Since in this orientation the field is approximately antiparallel to the direction of the cooling field, the energy term containing J_E can be absorbed into the Zeeman energy term according to our single domain

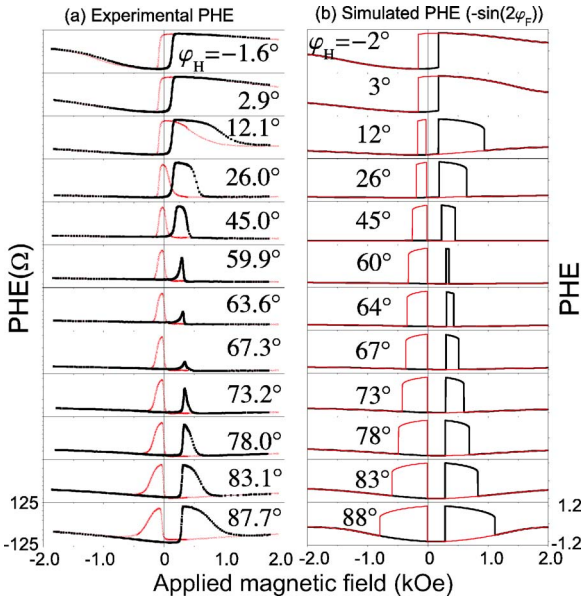

FIG. 3. (Color online) Planar Hall effect results obtained for the (Ga,Mn)As/MnO exchange-biased structure. Column (a) on the left shows experimental PHE data obtained at 4.2 K. The cooling field is along the $[1\bar{1}0]$ direction of the (Ga,Mn)As layer, and the direction of the applied magnetic field is at different azimuthal angles φ_H relative to the [110] direction, which is also the direction of the current. Column (b) is simulation of the PHE curves for the angle φ_H used in the experiments, obtained by assuming a single domain structure in the FM layer and frozen spins in the AF layer. Red (thinner) curves correspond to decreasing field branches, and black (thicker) curves correspond to increasing field branches.

model. Thus the PHE curve should in this case be the same as that in the case of "ordinary" PHE, i.e., typical of (Ga,Mn)As without an AF capping layer, except that the entire curve is shifted toward a positive field. The first jump in the PHE resistance in the center of the increasing-field branch corresponds to the switching of FM moments from the $[0\bar{1}0]$ ($\varphi_F \approx 225°$) to the $[\bar{1}00]$ ($\varphi_F \approx 135°$) direction (see Fig. 1 for definition of coordinates). We will refer to the field at which this occurs as the "first switching field," H_{S1}. Since $E_{\mathrm{DW}} = E(\varphi_F = 225°) - E(\varphi_F = 135°)$, it is straightforward—using Eq. (10c) and noting that $\varphi_H \approx \varphi_{\mathrm{CF}} + 180°$—to obtain the expression

$$\frac{E_{\mathrm{DW}}}{t_F M} \approx \frac{J_E}{t_F M}\left[\cos\left(\varphi_{\mathrm{CF}}-\frac{3}{4}\pi\right)-\cos\left(\varphi_{\mathrm{CF}}-\frac{5}{4}\pi\right)\right] + H_{S1}\left[\cos\left(\varphi_H-\frac{3}{4}\pi\right)-\cos\left(\varphi_H-\frac{5}{4}\pi\right)\right].$$

Using the value of H_{S1} from the experimental PHE data (270–290 Oe for φ_H close to 90°), we obtain $E_{\mathrm{DW}}/t_F M \sim 214$ Oe.

We must point out here that the value of E_{DW} determined in this way includes the effects of pinning at the inhomogeneous FM-AF interface. As indicated in Refs. 12 and 13, this pinning effect is more pronounced when the direction of the sweeping field is either parallel or antiparallel to the cooling

field direction than for other directions. Thus we can conclude that the above value of E_{DW} is not intrinsic to the (Ga,Mn)As layer. The intrinsic value of E_{DW} can be obtained from the PHE data obtained when the applied field direction is perpendicular to the cooling field direction, i.e., from the curve with $\varphi_H=-1.6°$, and should be smaller than the one determined above. One should note as well that, as concluded by Liu *et al.*,[32] the domain wall formation energy E_{DW} is proportional to $\sqrt{\Delta E}$, where ΔE is the height of the energy barrier between the two local energy minima (i.e., between the states just before and just after the switching of the direction of magnetization).

Although it appears that E_{DW} can vary in different situations, we argue that its value will not affect the EB field of the simulated loop, since in our model this shift is primarily determined by J_E and is relatively independent of E_{DW}. Consequently, for the purpose of obtaining H_{EB} itself, we can choose the value of E_{DW} somewhat arbitrarily. In the present analysis we will then choose to use the value of E_{DW} determined from the PHE curve for $\varphi_H=87.7°$. It must be emphasized, however, that E_{DW} is the key factor for determining the coercivity in our model, and later we will see that it can also affect the dependence of PHE on the direction of applied magnetic field.

C. Dependence of PHE on the angle of applied field in the presence of EB

PHE data obtained on the same $t_F=15$ nm sample at 4.2 K for the cooling field angle $\varphi_{CF}=-94°\pm2°$ are shown as a function of magnetic field in Fig. 3, with the applied magnetic field angle φ_H ranging from 0 to 90°. We show two columns of plots: column (a) contains experimental PHE data; and column (b) shows simulated PHE resistances computed from the simplified free energy given in Eq. (10c) for each field orientation in column (a). We recall from Eq. (2) that PHE varies as $-\sin(2\varphi_F)$, where the minus sign corresponds to the negative value of $(\rho_\parallel-\rho_\perp)$ assigned to (Ga,Mn)As (see Ref. 28). The values of the parameters used in the simulation have been listed earlier in this article (see Sec. IV B).

1. Comparison of simulation with experimental results

It is instructive to compare the results of the simulation with experimental data, as seen in Figs. 3(a) and 3(b), since this comparison provides valuable insights into the mechanisms governing PHE in the presence of exchange bias field.

(i) *PHE at small values of* φ_H ($\varphi_H\sim0°$). The top two panels of column (a) and column (b) in Fig. 3 correspond to $\varphi_H=-2°$ and 3°, respectively, i.e., when the applied magnetic field is nearly perpendicular to the cooling field. In this regime of φ_H, both experimental results and simulation show a clear single hysteresis shape in the PHE resistance. This feature is unique, since in a "bare" (Ga,Mn)As epilayer (i.e., one without the AF capping layer), such behavior can only be seen when the applied magnetic field is strictly along the hard axis (i.e., along the ⟨110⟩ orientations);[28] otherwise one will always see a "double-bump" feature. In our case, the presence of the exchange coupling allows us to observe this feature in a rather broad range of φ_H ($-5°\sim+5°$). Simulation shows that this is due to the fact that the unidirectional coupling confines the FM magnetization in the semiplane that contains the direction of the cooling field, so that the FM magnetization undergoes only one switching (in our case from $\varphi_F=225°$ to $\varphi_H=-315°$). In "bare" (Ga,Mn)As epilayers, however, even a small deviation of the applied magnetic field from the hard axis will result in a double-switching feature during the FM magnetization reversal from one saturated state to the other.

Finally, at small angles φ_H we see relatively narrower loops in the experimental results compared to those in the simulation. This is believed to arise from the fact that when the FM magnetization passes the direction of the cooling field during magnetization reversal, the inhomogeneous interfacial coupling has the least effect on the movement of the magnetization. The switching is then chiefly governed by the intrinsic value of E_{DW} of (Ga,Mn)As.[12,13]

(ii) *Critical angle of applied magnetic field.* When φ_H increases above 3°, we see that the magnetic field dependence of PHE resistance gradually evolves into a bump in the decreasing and the increasing branches both in experimental results and in simulations. Another striking feature seen in Fig. 3 is that the resistance bump in the increasing field branch rapidly becomes narrower with increasing φ_H up to some angle ($\varphi_H\approx67°$ in experimental data, and 60° in the simulation), after which it again begins to broaden. The simulation reproduces this feature encouragingly well, except for the exact value of this special angle. We will refer to this angle as the "critical angle," denoted by φ_{HC}.

The occurrence of such critical angle can be understood by examining the calculated behavior of the orientation of magnetization φ_F shown in Figs. 4 and 5. When $\varphi_H\leqslant\varphi_{HC}$ (Fig. 4), in the increasing field branch φ_F first goes to 225° (i.e., **M** aligns along the $[0\bar{1}0]$ easy-axis direction), then to 315° (by domain nucleation and expansion), i.e., **M** is reoriented to point along [100]; and then to 45° ($\mathbf{M}\parallel[010]$); and eventually **M** will turn to the field direction, $\varphi_F\rightarrow\varphi_H$. After saturation by a positive field, as the field decreases, the angle φ_F first returns to 45°; then rotates to 315°; and finally to 225°. We will refer to this type of magnetization reversal process as "half circle" rotation of **M**. In the figure, the symbols I and II represent the first and second switching states in the increasing field branch, and III and IV are the first and second switchings in the decreasing field branch. The path is different when $\varphi_H>\varphi_{HC}$ (Fig. 5), since in this case the magnetization angle φ_F undergoes a full 360° rotation in completing the hysteresis loop, and we will refer to the process depicted in Fig. 5 as a "full circle" reversal.

As pointed out earlier, the route which the FM moments choose to complete the hysteresis loop is determined by the behavior of the free energy of the system as the field is swept. To clarify this point, we examine the free energy plots for switching state I in the two cases (i.e., $\varphi_H\leqslant\varphi_{HC}$ and $\varphi_H>\varphi_{HC}$). We can see that the FM moments reorient to 315° in Fig. 4 and to 135° in Fig. 5, since these orientations of **M** correspond, respectively, to the lowest energy states adjacent to the 225° orientation of **M**. Actually, as φ_H is changed from 0° to 90°, for switching state I the energy for $\varphi_F=315°$ in-

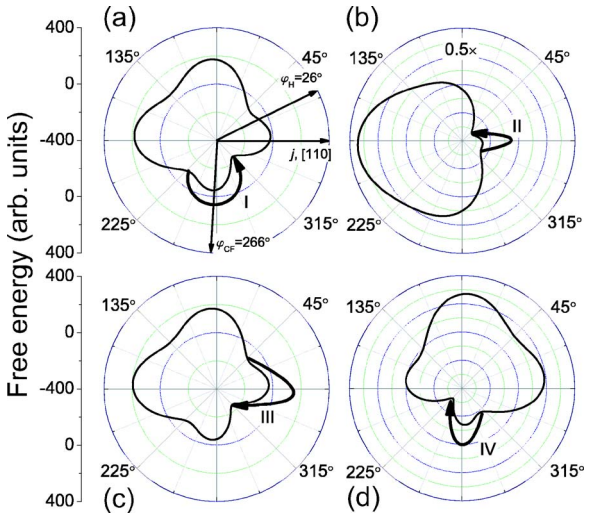

FIG. 4. (Color online) Plots of the free energy of the system as a function of the direction of FM magnetization φ_F at the four switching fields for the applied field angle φ_H=26°. (a), (b), (c) and (d) correspond to switchings I, II, III, and IV, respectively, as defined in the text, with the solid curvy arrow in each panel showing how the magnetization reorients at each switching. Note that reorientation is always by 90°, along the path with the lowest energy barrier.

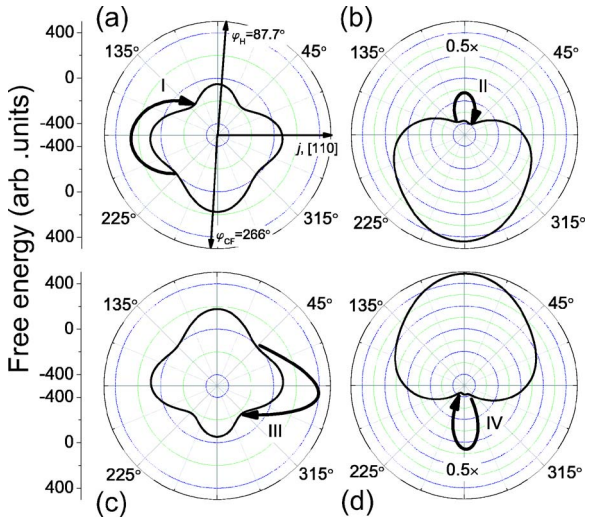

FIG. 5. (Color online) Plots of the free energy of the system as a function of the direction of FM magnetization φ_F at the four switching fields for the applied field angle φ_H=87.7°. (a), (b), (c) and (d) correspond to switchings I, II, III, and IV, respectively, as defined in the text, with the solid curvy arrow in each panel showing how the magnetization reorients at each switching. Note that reorientation is always by 90°, along the path with the lowest energy barrier.

creases, while the energy for φ_F=135° decreases, so that it gradually becomes harder for the FM moments to remain at the 315° orientation after switching I. Intuitively, this suggests that the time in which **M** can remain at 315° during the field sweep becomes increasingly shorter. This explains why the resistance bump in the increasing field branch becomes narrower first; and at some certain angle φ_H—at which $E(\varphi_F=135°)=E(\varphi_F=315°)$—the width of this bump nearly vanishes. After φ_H passes this critical angle, the FM moments begin to strongly favor φ_H=135° for their first jump, and tend to remain at 135° for a longer time during the field sweep. This explains the increasing width of the bump in the increasing field branch when $\varphi_H > \varphi_{HC}$.

Returning to the critical angle φ_{HC}, its value can be estimated in the following way based on our single domain model. At the critical angle $\varphi_H=\varphi_{HC}$ we have

$$E_{DW} = E(\varphi_F = 225°) - E(\varphi_F = 135°)$$
$$= E(\varphi_F = 225°) - E(\varphi_F = 315°),$$

from which we can easily derive the expression for φ_{HC}:

$$\varphi_{HC} \approx \arctan\left(\frac{E_{DW} - J_E\left[\cos\left(\varphi_{CF} - \frac{3}{4}\pi\right) - \cos\left(\varphi_{CF} - \frac{5}{4}\pi\right)\right]}{E_{DW} - J_E\left[\cos\left(\varphi_{CF} - \frac{7}{4}\pi\right) - \cos\left(\varphi_{CF} - \frac{5}{4}\pi\right)\right]}\right), \quad \left(0 \leqslant \varphi_H \leqslant \frac{\pi}{2}\right). \tag{11}$$

If J_E/Mt_F=140 Oe and E_{DW}/Mt_F=214 Oe, as determined previously in this article, we obtain φ_{HC}=61°. The deviation of this value from the experimentally observed φ_{HC}=67° probably comes from the uncertainty in the value of E_{DW}. For φ_H in other quadrants, the calculated critical angles can be obtained in a similar way.

2. Outside the scope of the model

Although the agreement between experimental results and the simulation is encouraging, differences are inevitably encountered since the model we used is relatively naive. Specifically, it assumes a uniform effective exchange coupling at the interface, a single domain structure in the FM layer, and a constant value of E_{DW} independent of φ_H. Actually, the interface between the AF layer and the FM layer cannot be perfect, and a uniform exchange coupling is an oversimplification aimed at obtaining a zeroth-order picture. A more realistic model, that includes inhomogeneous coupling at the AF-FM interface, will result in mutidomain structures in the FM layer, which will in turn lead to enhancement of

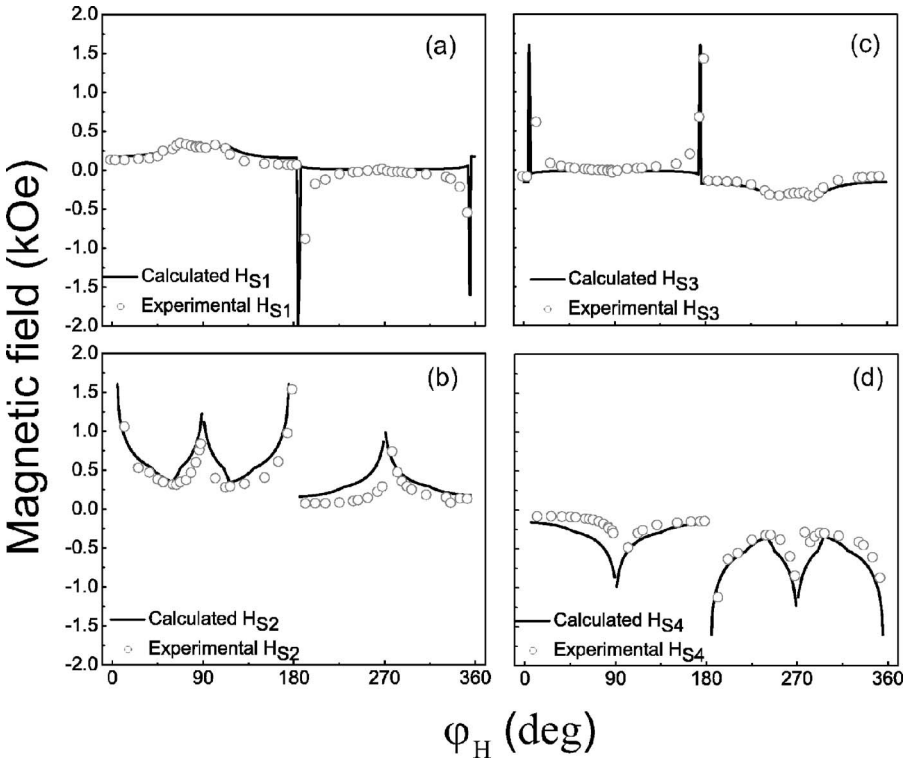

FIG. 6. Plots of the four switching fields as a function of the applied magnetic field orientation. The open circles are experimental data, and the solid curves are simulations. (a), (b), (c), and (d) correspond to switchings I, II, III, and IV, respectively.

coercivity[5,12,14] and smoothing out the PHE curves at points corresponding to switchings of magnetization direction.

(i) *Asymmetry seen in experimental PHE curves at* $\varphi_H \rightarrow 90°$. When the angle of applied magnetic field is approaching 90° (i.e., the hard direction of the FM layer), an asymmetry is observed in the experimental PHE curves, i.e., the width of the "bump" observed in the increasing-field branch [black curve in the bottom panel in Fig. 3(a)] is significantly greater than the bump width seen in the decreasing branch (red curve). Our single domain model is not able to reproduce this, since in the simulated PHE curves as $\varphi_H \rightarrow 90°$ [bottom panel in Fig. 3(b)], i.e., the widths of the bumps are equal in both branches. This is easy to understand, because in our model—when the magnetic field is applied either parallel or antiparallel to the direction of the cooling field—the exchange coupling simply plays the role of an effective field that is added or subtracted to the applied field, and its effect will only be to shift the PHE curve relative to the zero field, without affecting the separation between magnetization switchings. It is possible that this observed asymmetry in PHE is related to that seen in the SQUID data (discussed in Sec. IV A), where we suggested that the effect arises from the inhomogeneous coupling at the FM-AF interface.[45]

(ii) *Smoothing-out of the switching of magnetization in (Ga,Mn)As*. The inhomogeneous interfacial coupling will lead the FM layer into a multidomain state, with different domains reorienting at different applied field during the sweep since each domain is affected by a different coupling field from the AF layer. We must note here, however, that the much smoother behavior of switching II and IV compared to switching I and III is not unique to our EB systems, and is also seen in "bare" (Ga,Mn)As epilayers as discussed by Shin *et al.*[39] In their argument, for switching II and IV multidomain structures in the FM layer are more likely to form than for switchings I and III. Since in our exchange-biased systems a multidomain landscape is more prevalent to begin with (due to inhomogeneous FM-AF coupling across the interface), and the switchings observed are decidedly much smoother than in non-EB layers, the increased smoothing which we observe appears to reinforce the arguments of Shin *et al.*

D. Dependence of switching fields and EB field on φ_H

For completeness, we plot in Fig. 6 the observed and simulated angular dependences of the fields at which the magnetization switchings I, II, III, and IV take place, designated as H_{S1}, H_{S2}, H_{S3}, and H_{S4}, respectively. As usual, the switching fields are defined as fields at which the corresponding PHE curve intersects the field axis (i.e., the x axis). The good agreement between all trends of the switching fields obtained from simulation and from experiment indicates that the single domain model is quite useful as a preliminary attempt of identifying the underlying mechanisms that govern the process of magnetization reversal in the FM layer in the presence of exchange coupling.

Some quantitative deviations between the calculated results and the experimental data are nevertheless observed in certain regions. For instance, in Figs. 6(a) and 6(c) deviation is quite apparent in the region near the "spike;" and in Figs. 6(b) and 6(d) some disagreement is seen in the regions near 270° and 90°. The deviations in Figs. 6(b) and 6(d) are likely due to our inability to achieve a perfect alignment of the magnetic field with the sample axes. We are less clear about the origin of the discrepancies seen in Figs. 6(a) and 6(c). One possible reason is that we use a constant domain wall energy for the FM layer, while in reality this energy can vary.

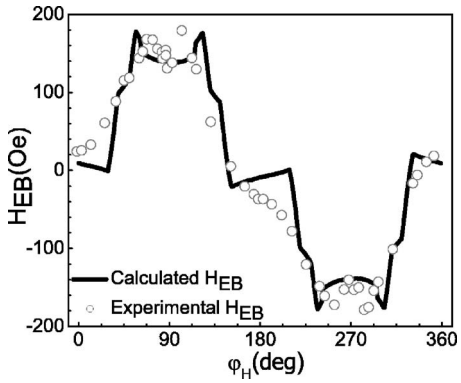

FIG. 7. Plots of the exchange bias field as a function of the applied magnetic field orientation. The open circles are determined from experimental PHE curves, and the solid curve is from simulations.

Another factor is of a more practical nature, arising from the difficulty in precisely locating the actual fields in the experimental data due to the rather smooth shape of the transitions in the PHE curves that result from the multidomain structure in the FM layer.

In Fig. 7 we also plot the dependence of the exchange bias H_{EB} with respect to φ_H, obtained both from the experimental results and from simulation. The definition of H_{EB} is given by $H_{EB}=(H_{CI}+H_{CD})/2$, where H_{CI} and H_{CD} are coercive fields in the increasing- and decreasing-field branches, respectively, i.e., the two intercepts of the magnetization hysteresis loop with the field axis. From the computed magnetization curve it is easy to determine these coercive fields. The situation becomes complicated, however, when one deals with the experimental PHE curves, since the multidomain structure in our FM layer makes the determination of coercive fields nearly impossible at some angles of the applied magnetic field. To make some progress, we will therefore impose the single-domain assumption also for the purpose of locating the experimental coercive fields as follows. In the single domain situation, H_{CI} or H_{CD} is the field at which the magnetization is perpendicular to the magnetic field, i.e., $\varphi_F-\varphi_H=\pm 90°$, and by recalling the definition of R_{PHE} given in Eq. (2), we can write

$$R_{PHE}=-R_{Amp}\sin(2\varphi_F)=-R_{Amp}\sin[2(\varphi_F-\varphi_H)+2\varphi_H],$$

where R_{Amp} is the amplitude of the PHE resistance (half height of the R_{PHE} bump). Using the definition that at H_{CI} and H_{CD}, $\varphi_F-\varphi_H=\pm 90°$, we obtain the PHE resistance corresponding to the coercive fields, $R^C_{PHE}=R_{Amp}\sin(2\varphi_H)$. Thus the experimental coercive field is just that corresponding to the intercept of the experimental PHE curve with the horizontal line determined by $R^C_{PHE}=R_{Amp}\sin(2\varphi_H)$.

We can see that the agreement is also acceptable, although at $\varphi_H\approx 0°$ and $\varphi_H\approx 180°$ some deviation is observed. Bearing in mind that we are making the single domain assumption not only to do the simulation, but also to determine the coercive fields from experimental PHE data, the agreement is quite encouraging.

Finally, since the weakness of the single-domain model lies in its inability to account for the coercivity enhancement that accompanies exchange bias, discussing other aspects of coercivity in terms of this model (such as angular dependence of the coercivity) is not likely meaningful. It is clear that a more comprehensive model, which includes variation of E_{DW} and allows for a multidomain structure in the FM layer, will be needed to deal with magnetic coercivity in exchange-biased systems.

V. CONCLUSIONS

In this paper we have studied the exchange coupling in a bilayer structure comprised of an FM (Ga,Mn)As layer and an AF MnO capping layer. The presence of exchange bias in our sample was determined from direct magnetization measurements, which provides the value of the exchange bias field H_{EB}. An effective interfacial coupling constant J_E was then obtained from the observed exchange bias field, which allowed us to estimate the deviation of the AF moments from the direction of cooling field is negligibly small. This provides grounds for the assumption that the AF spins are frozen during magnetization reversal in the (Ga,Mn)As layer.

We then carried out a systematic series of PHE measurements on an exchange-biased (Ga,Mn)As/MnO system as a function of the applied field and its orientation. Using a model which assumes frozen AF spins, a single domain in the FM layer, and a constant value of the domain wall energy E_{DW} for the FM layer, magnetic field dependence of the PHE resistance was simulated and compared with experimental PHE results. We have shown that the single domain model can account for the hysteresis shape of PHE curves when the applied magnetic field is perpendicular to the cooling field and along the hard direction of the FM layer, and for the appearance of the critical angle of the applied magnetic field. Agreement between the switching fields and EB fields obtained from the experimental results and from the simulation further confirms the effectiveness of our model. On the other hand, since the current model is too simple to account both for the asymmetric behavior of the hysteresis loop and for the behavior of the coercivity, it is our hope that the results presented in this paper will stimulate further attention—both theoretical and experimental—to this aspect of exchange biased ferromagnetic semiconductors.

ACKNOWLEDGMENTS

The authors thank B. Kirby for carrying out the XRR measurements on our samples. The authors also express their thanks to S. Lee for very instructive discussions. This work was supported by NSF Grants No. DMR02-10519 and No. DMR06-03752.

*Electronic address: mdobrowo@nd.edu

[1] W. H. Meiklejohn and C. P. Bean, Phys. Rev. **102**, 1413 (1956); **105**, 904 (1957).
[2] D. Heim, R. Fontana, C. Tsang, V. Speriosu, B. Gurney, and M. Williams, IEEE Trans. Magn. **30**, 316 (1994).
[3] J. Nogués and I. K. Schuller, J. Magn. Magn. Mater. **192**, 203 (1999).
[4] M. Kiwi, J. Magn. Magn. Mater. **234**, 584 (2001).
[5] M. D. Stiles and R. D. McMichael, Phys. Rev. B **59**, 3722 (1999).
[6] K. Takano, R. H. Kodama, A. E. Berkowitz, W. Cao, and G. Thomas, Phys. Rev. Lett. **79**, 1130 (1997).
[7] D. Mauri, H. C. Siegmann, P. S. Bagus, and E. Kay, J. Appl. Phys. **62**, 3047 (1987).
[8] H. Xi and R. M. White, Phys. Rev. B **61**, 80 (2000).
[9] A. P. Malozemoff, Phys. Rev. B **35**, 3679 (1987); **37**, 7673 (1988); J. Appl. Phys. **63**, 3874 (1988).
[10] P. Miltényi, M. Gierlings, J. Keller, B. Beschoten, G. Güntherodt, U. Nowak, and K. D. Usadel, Phys. Rev. Lett. **84**, 4224 (2000).
[11] S. Zhang, D. V. Dimitrov, G. C. Hadjipanayis, J. W. Cai, and C. L. Chien, J. Magn. Magn. Mater. **198**, 468 (1999).
[12] Z. Li and S. Zhang, Phys. Rev. B **61**, R14897 (2000).
[13] Z. Li and S. Zhang, Appl. Phys. Lett. **77**, 423 (2000).
[14] M. D. Stiles and R. D. McMichael, Phys. Rev. B **63**, 064405 (2001).
[15] H. Ohno, Science **281**, 951 (1998).
[16] T. Dietl, H. Ohno, and F. Matsukura, Phys. Rev. B **63**, 195205 (2001).
[17] A. H. MacDonald, P. Schiffer, and N. Samarth, Nat. Mater. **4**, 195 (2005).
[18] X. Liu, Y. Sasaki, and J. K. Furdyna, Phys. Rev. B **67**, 205204 (2003).
[19] U. Welp, V. K. Vlasko-Vlasov, X. Liu, J. K. Furdyna, and T. Wojtowicz, Phys. Rev. Lett. **90**, 167206 (2003).
[20] X. Liu, Y. Sasaki, and J. K. Furdyna, Appl. Phys. Lett. **79**, 2414 (2001).
[21] J. K. Furdyna, X. Liu, Y. Sasaki, S. J. Potashnik, and P. Scheiffer, J. Appl. Phys. **91**, 7490 (2002).
[22] K. F. Eid, M. B. Stone, O. Maksimov, T. C. Shih, K. C. Ku, W. Fadgen, C. J. Palmstrøm, P. Schiffer, and N. Samarth, J. Appl. Phys. **97**, 10D304 (2005).
[23] B. H. Miller and E. D. Dahlberg, Appl. Phys. Lett. **69**, 3932 (1996).
[24] C. Leighton, M. Song, J. Nogués, M. C. Cyrille, and I. K. Schuller, J. Appl. Phys. **88**, 344 (2005).
[25] J. B. Yi, J. Ding, B. H. Liu, Z. L. Dong, T. White, and Y. Liu, J. Magn. Magn. Mater. **285**, 224 (1999).
[26] G. Li, T. Yang, Q. Hu, H. Jiang, and W. Lai, Phys. Rev. B **65**, 134421 (2002).
[27] J. P. Pan, *Solid State Physics*, edited by F. Seitz and D. Tirnbull (Academic, New York, 1957), Vol. 5, pp. 1–96.
[28] H. X. Tang, R. K. Kawakami, D. D. Awschalom, and M. L. Roukes, Phys. Rev. Lett. **90**, 107201 (2003).
[29] W. L. Lim, X. Liu, K. Dziatkowski, Z. Ge, S. Shen, J. K. Furdyna, and M. Dobrowolska, J. Appl. Phys. **99**, 08D505 (2006).
[30] I. Kuryliszyn-Kudelska, J. Z. Domagala, T. Wojtowicz, X. Liu, E. Lusakowska, W. Dobrowolski, and J. K. Furdyna, J. Appl. Phys. **95**, 603 (2004).
[31] B. Kirby (private communication).
[32] X. Liu, W. L. Lim, L. V. Titova, M. Dobrowolska, J. K. Furdyna, M. Kutrowski, and T. Wojtowicz, J. Appl. Phys. **98**, 063904 (2005).
[33] T. Dietl, J. Konig, and A. H. MacDonald, Phys. Rev. B **64**, 241201(R) (2001).
[34] C. Leighton, J. Nogués, B. J. Jösson-Åkerman, and I. K. Schuller, Phys. Rev. Lett. **84**, 3466 (2000).
[35] M. Farle, Rep. Prog. Phys. **61**, 755 (1998).
[36] Joo-Von Kim, R. L. Stamps, B. V. McGrath, and R. E. Camley, Phys. Rev. B **61**, 8888 (2000).
[37] H. Xi, K. R. Mountfield, and Robert M. White, J. Appl. Phys. **87**, 4367 (2000).
[38] K. Hamaya, T. Taniyama, Y. Kitamoto, R. Moriya, and H. Munekata, J. Appl. Phys. **94**, 7657 (2003).
[39] D. Y. Shin, S. J. Chung, S. Lee, X. Liu, and J. K. Furdyna (unpublished).
[40] M. S. Jagadeesh and M. S. Seehra, Phys. Rev. B **23**, 1185 (1981).
[41] X. W. Wu and C. L. Chien, Phys. Rev. Lett. **81**, 2795 (1998).
[42] Z. Ge, W. L. Lim, Y. J. Cho, Y. Y. Zhou, X. Liu, J. K. Furdyna, and M. Dobrowolska, IEEE Trans. Magn. (to be published).
[43] M. R. Fitzsimmons, P. Yashar, C. Leighton, I. K. Schuller, J. Nogués, C. F. Majkrzak, and J. A. Dura, Phys. Rev. Lett. **84**, 3986 (2000).
[44] J. Camarero, J. Sort, A. Hoffmann, J. M. García-Martín, B. Dieny, R. Miranda, and J. Nogués, Phys. Rev. Lett. **95**, 057204 (2005).
[45] Z-P. Li, O. Petracic, R. Morales, J. Olamit, X. Batlle, K. Liu, and I. K. Schuller, Phys. Rev. Lett. **96**, 217205 (2006).
[46] W.-T. Lee, S. G. E. te Velthuis, G. P. Felcher, F. Klose, T. Gredig, and E. D. Dahlberg, Phys. Rev. B **65**, 224417 (2002).
[47] E. Pina, C. Prados, and A. Hernando, Phys. Rev. B **69**, 052402 (2004).
[48] M. Gierlings, M. J. Prandolini, H. Fritzsche, M. Gruyters, and D. Riegel, Phys. Rev. B **65**, 092407 (2002).
[49] A. Hoffmann, Phys. Rev. Lett. **93**, 097203 (2004).
[50] B. A. Coles, J. W. Orton, and J. Owen, Phys. Rev. Lett. **4**, 116 (1960).
[51] J. van Lierop, M. A. Schofield, L. H. Lewis, and R. J. Gambino, J. Magn. Magn. Mater. **264**, 146 (2003).
[52] F. Keffer and W. O'Sullivan, Phys. Rev. **108**, 637 (1957).